

A Metamaterial Inspired UWB Antenna for WLAN Application

Ambica Yadav¹, Sovan Mohanty²P.G. Student, Department of Electronics & Communication, Shri Ram Murti Smarak College of Engg. & Technology
Bareilly, India¹Associate Professor, Department of Electronics & Communication, Shri Ram Murti Smarak College of Engg. &
Technology Bareilly, India²

ABSTRACT: A new compact ultra wideband (UWB) microstrip inverted T-slotted antenna based on composite right/left handed materials is proposed here. Metamaterials are artificial structures with properties that may not be found in nature. Since their initial advent, they have inspired ground-breaking applications to a range of research topics, such as electromagnetic invisibility of objects (cloaking), radiation absorption, filtering of light and sound as well as efficient antennas for sensors and implantable communication devices in recent years. The antenna structure is so designed that it operates in the range of (3.1-10.6 GHz) and had a resonance at 5.5GHz WLAN. The total footprint of the antenna is taken to be $0.46 \lambda_0 \times 0.38 \lambda_0 \times 0.029 \lambda_0$, where λ_0 is free space wavelength. The designed prototype had a wider bandwidth of 1000MHz and a minimum value of reflection of -28.59dB in the structure. The proposed UWB antenna had a gain of 3.5dB, and a minimum value of VSWR, which is considered to be optimum for a good performance antenna.

KEYWORDS: UWB, metamaterial, SRR's.

I. INTRODUCTION

Metamaterials are artificial materials engineered to provide properties which “may not be readily available in nature”. These materials usually gain their properties from structure rather than composition, using the inclusion of small inhomogeneities to enact effective macroscopic behaviour. The metamaterials have entered into the main stream of electromagnetics. The essential property in metamaterials is their unusual and desired qualities that appear due to their particular design & structure. In particular composite media electromagnetic waves interact with the inclusions which produce electric & magnetic moments, which in turn affect the macroscopic effective permittivity & permeability of the bulk composite medium. Since metamaterials can be synthesized by embedding artificially fabricated inclusions in a specified host medium. This provides the designer with a large collection of independent parameters such as properties of host materials, size, shape, and compositions of inclusions. All these design parameters can play a major role in getting the final result. In these the shape of the inclusions is one that provides a new possibility for metamaterial processing.

In electromagnetism, electric permittivity (ϵ), and magnetic permeability (μ) are the two fundamental parameters characterizing the EM property of a medium. Physically, permittivity (permeability) describes how an electric (magnetic) field affects, and is affected by a medium, which is determined by the ability of a material to polarize in response to the electric (magnetic) field. We use the “material parameter space” as shown in Fig. 1 to represent all materials, as far as EM properties are concerned. Region I in the upper right quadrant covers materials with simultaneously positive permittivity and permeability, which include most dielectric materials. Quadrant II embraces metals, ferroelectric materials, and doped semiconductors that could exhibit negative permittivity at certain frequencies (below the plasma frequency). Region IV is comprised of some ferrite materials with negative permeability, the magnetic responses of which, however, quickly fade away above microwave frequencies. The most interesting region

International Journal of Innovative Research in Science, Engineering and Technology

(An ISO 3297: 2007 Certified Organization)

Vol. 5, Issue 6, June 2016

in the material parameter space is quadrant III, in which permittivity and permeability are simultaneously negative. In nature there is no such material.

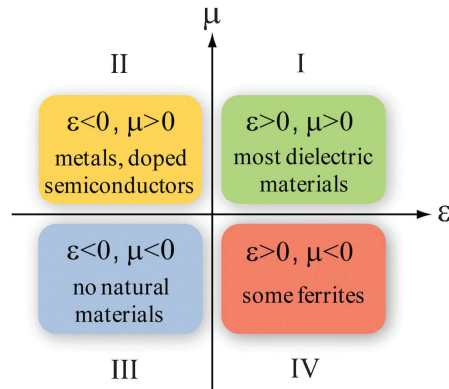


Figure 1: Material parameter space characterized by electric permittivity (ϵ) and magnetic permeability (μ).

II. RELATED WORK

Since 2002, numerous SRRs having various geometrical configurations have been proposed. However, most of these SRRs are derived from the prototype structure proposed in. For example, a square split ring resonator (S-SRR) was proposed which has more degrees of freedom from a design point of view, and more magnetic coupling with the host transmission line, than SRRs. Saha *et al.* built a theoretical model for S-SRRs to estimate their resonant frequency and their magnetic polarization. They also investigated the bandstop behavior of these resonators when loaded into CPW. In, bandstop filters based on SRRs placed on the back side of CPW substrate were first introduced. These filters give significant insertion loss in the rejection band with very good frequency selectivity near the resonant frequency. A spiral resonator of one metallic planar piece is proposed in order to facilitate the fabrication process because of the absence of the narrow slots between the strips. A modified broadside coupled SRR was proposed by Marques *et al.* as an alternative to a conventional SRR in order to avoid the bi-anisotropic effects.

Several numerical and analytical methods were introduced to characterize the constitutive parameters for AMMs (artificial magnetic metamaterials). Smith and Pendry proposed a field averaging method in order to homogenize a periodic structure that contains several metamaterial cells with different geometries. The electric and magnetic fields were averaged and calculated at the edges of two successive cubic lattices. The effective parameters of a transmission line loaded with asymmetrical SRRs were calculated by proposing an equivalent bi-anisotropic medium, which imitates the effect of asymmetric unit cells. Analytical expressions for the relative permittivity and permeability of SRRs were introduced based on a simple transmission line theory. The two parameters were extracted from the derived expressions of reflection and transmission coefficients. Effective material parameters in metamaterial were calculated using a modal approach combined with the Finite Integration Technique (a generalized FDTD method). The parameter fitting of dispersive models (PFDMs) method was used to extract the effective material parameters from the scattering parameters of a double negative metamaterial structure.

The second approach to produce metamaterial-based components and circuits is a non-resonant artificial transmission lines-based approach called composite right/left handed transmission lines. Their nonlinear phase slope response makes them convenient to produce arbitrary dual-band circuits by simply replace the conventional lines in prototype circuits. A two-dimensional (2-D) CRLH TLs have been investigated. Their dispersive diagram has been derived analytically. Similar planar cells were utilized to produce infinite wavelength resonant antennas with monopolar radiation patterns.

International Journal of Innovative Research in Science, Engineering and Technology

(An ISO 3297: 2007 Certified Organization)

Vol. 5, Issue 6, June 2016

Other 2-D planar resonant-type distributed structure based on complimentary split ring resonators and series gap capacitors has been proposed.

III. ENGINEERING ELECTRIC AND MAGNETIC RESPONSES BY METAMATERIALS

In classical electromagnetics, usually the material property can be well described by the Drude–Lorentz model, which can be derived from the oscillation equation of electric charges or fictitious magnetic charges driven by an external EM wave. Due to the symmetry of EM waves, the frequency-dependent permittivity and permeability follow very similar formula,

$$\begin{cases} \epsilon_r(\omega) = 1 - \frac{\omega_{p,e}^2}{\omega^2 - \omega_{0,e}^2 + i\gamma_e\omega} \\ \mu_r(\omega) = 1 - \frac{\omega_{p,m}^2}{\omega^2 - \omega_{0,m}^2 + i\gamma_m\omega} \end{cases}$$

Here ω_p is the plasma frequency, ω_o is the resonant frequency, and γ is the damping factor related to material losses. The subscripts e and m represent electric and magnetic response.

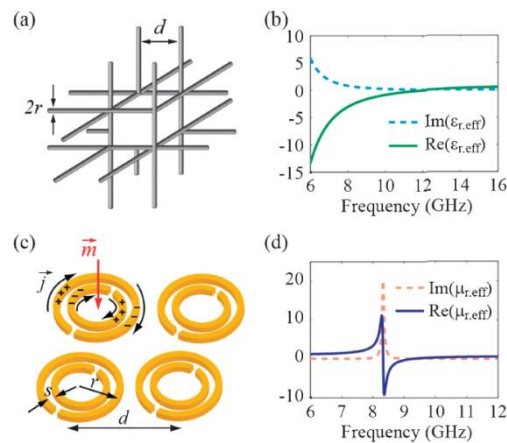


Figure 2: Basic metamaterial structures to implement artificial electric and magnetic responses. (a) Schematic of periodic wires (with radius r) arranged in a simple cubic lattice (with lattice constant d). (b) Effective permittivity of wire media, acting as dilute metals with an extremely low plasma frequency. (c) Schematic of split ring resonators, with outer radius r and separation s between the two rings. A magnetic field penetrating the resonator induces a current (j), and thus a magnetic moment (m). (d) Effective permeability of split ring resonators around the resonance frequency.

respectively. Substituting proper values into equation above, we can characterize material properties over a wide frequency range from microwave to optical. For noble metals, $\omega_{p,e}$ is at visible or UV frequency and $\omega_{0,e}$ is taken as zero under the free electron approximation. This means that the permittivity of metals is always negative below the plasma frequency. On the other hand, naturally existing materials that exhibit magnetic responses with negative permeability are far less common than those that exhibit electric responses. This is particularly true when we move beyond the gigahertz region, where the magnetic response of most materials begins to tail off. The fundamental reason for rare magnetic materials at high frequencies is that magnetic polarization originates from either the flow of orbital

International Journal of Innovative Research in Science, Engineering and Technology

(An ISO 3297: 2007 Certified Organization)

Vol. 5, Issue 6, June 2016

currents or unpaired electron spins, but both effects only respond to EM waves at low frequencies.⁹ In the optical regime, $m = 1$ holds for all naturally existing materials.

IV. NEGATIVE INDEX METAMATERIAL AND APPLICATIONS OF METAMATERIALS

By overlapping two sets of meta-structures with $\epsilon_{r,eff} < 0$ and $\mu_{r,eff} < 0$ in the same frequency window, we expect to create metamaterials with a negative effective refractive index (i.e., $n_{eff} < 0$), which were first experimentally demonstrated by Smith and colleagues in the microwave domain. A wedge-shaped metamaterial sample consisting of periodic array of copper SRRs and wires was used to measure the refraction of a beam at the exit interface (Fig. 3(a)). Negative refraction was indeed observed in a manner consistent with Snell's law. Although there were fierce debates on the validity of the experimental results as well as the fundamental properties of NIMs, a series of experimental and theoretical work ambiguously prove the reality of NIMs. Ever since then, considerable interest has been sparked in the field of metamaterials. Within several years, magnetic metamaterials, and consequently NIMs have been advanced from microwave frequencies to the visible region, by scaling down the structure size and taking prudent designs. Negative permeability is the heart of NIMs. To achieve magnetic resonance at optical frequencies, however, it is shown that the size of SRRs has to be smaller than 100 nanometers, and the gap is less than 10 nanometers. Furthermore, the amplitude of the resonant permeability from SRRs decreases and ultimately ceases to reach a negative value in the visible region. These challenges impelled researchers to seek alternative designs other than the combination of metallic wires and SRRs. The most successful optical NIMs so far are the fishnet structure, which consists of two layers of metal meshes separated by a dielectric spacer layer (Fig. 3(b)). The paired stripes that are oriented parallel to the electric field provide negative $\epsilon_{r,eff}$, while the other pairs of stripes parallel to the magnetic field offer negative $\mu_{r,eff}$. Since the thickness of the spacing dielectric is easy to control, the simple design of the fishnet structure significantly eases the fabrication burden, compared to the conventional approach of combing SRRs and metallic wires. In addition, the EM waves are incident normal to the fishnet sample surface to produce the negative refractive index. This configuration is much easier than that for NIMs based on SRRs and wires, which require oblique incidence of EM waves to excite SRRs with out-of-plane magnetic fields for strong magnetic resonances.

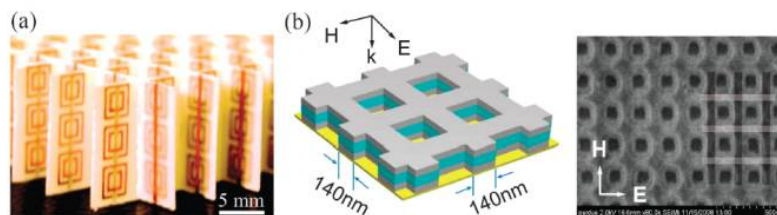


Figure 3: (a) NIMs working at microwave frequencies, which consist of copper SRRs and wires deposited lithographically on standard circuit boards. The size of the unit cell is 5 mm. Reprinted from ref. 15 with permission. (b) Fishnet structure as NIMs in the visible region (yellow light). The left panel is the schematic of the fishnet structure, in which two layers of metal mesh (gray) are separated by a dielectric layer (cyan). The right panel is the scanning electron microscope (SEM) image of the sample fabricated by electron beam lithography (EBL).

V. METAMATERIAL UWB ANTENNA

A. DESIGN CONSIDERATIONS

A simple microstrip patch antenna is designed to resonate at 5.5GHz. The overall size of the antenna was $25 \times 21 \times 1.6 \text{ mm}^3$. The radiating patch on the top layer is taken to be of length 15.41mm and 11.31mm of width. A T-slot is introduced in the center of the rectangular patch, and the 4 edges of the radiating patch was etched with 4 slots, all the edges of the patch was etched with a slot of width 1mm and length of 4mm in the top and 1mm width and 5mm length in the bottom of the rectangular patch. The dimensions of the inverted T-slot are as follows: the vertical slot is

International Journal of Innovative Research in Science, Engineering and Technology

(An ISO 3297: 2007 Certified Organization)

Vol. 5, Issue 6, June 2016

taken to be 6mm, and the horizontal slot of 2mm, the widths of the two slots are taken to be 2mm. The effects of T-slot and inverted T-slot as radiating patch. In, introducing complementary T slotted patch in the structure helped in achieving dual bands of operation. The upper inverted-T helped in achieving the band of 5.8GHz, here instead using metallic slot, the patch was etched to achieve the accurate band resonance of 5.5GHz, which is the frequency of operation for WLAN applications, which has a wider bandwidth.

Introducing slots in the radiating patch helps in improving the performance of an antenna. The design prototype is shown in figure 1. Figure 1(a) & (b) shows the top view of the structure and the bottom layer of the proposed antenna. The T slot in the center of the radiating patch was placed in such a way that the two perpendicular slots helped in resonating at the desired frequency range 5.5GHz. This resonating frequency states that the proposed antenna is applicable for the second generation of WLAN frequency band (5-6GHz). In this operating band, the bandwidth will be larger and can be helpful in allocating more number of users. This band is applicable for the applications like Bluetooth, Wi-Fi which are also having the frequency range of 2.2-2.8 GHz, with a narrow bandwidth. Since the lower frequency (f_1) of the operating band starts from 3.6GHz with a minimum return loss and the upper frequency (f_2) of the band was 10 GHz, this operating band was considered to be the range for Ultra-Wideband (UWB) frequencies, which are recently gaining more interest in real time applications. Since it offers more bandwidth, it helps in reduction of cross interference between the channels.

B. SRR's in the structure

The prototype was proposed using split ring resonators (SRR's). The SRR's may take various shapes in which here square shaped SRR's are considered. The SRR's basically consists of two loops: a smaller loop incorporated within the bigger one, with slots incorporated onto each at opposite ends. The SRR is a magnetically resonant structure that responds to a perpendicular magnetic field, which can be used to create negative permeability, gaps added to the rings introduces capacitance effect, which allows control in the resonant characteristic of the structure.

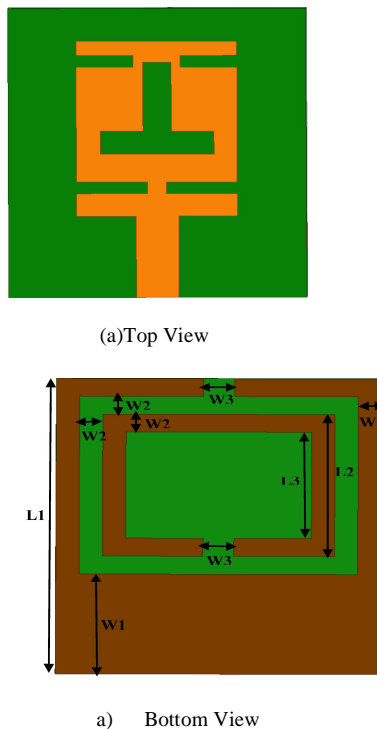


Figure 4: Prototype of the proposed structure

International Journal of Innovative Research in Science, Engineering and Technology

(An ISO 3297: 2007 Certified Organization)

Vol. 5, Issue 6, June 2016

The dimensions of the ring are taken as: $L1 = 25\text{mm}$, $L2 = 12\text{mm}$, $W1 = 8.5\text{mm}$, $W2 = 1.5\text{mm}$, $W3 = 2\text{mm}$. The partial ground plane and the outer loop of the ring are coupled together in order to increase the coupling effect.

VI. RESULT AND DISCUSSIONS

Here FR-4 is used as the dielectric medium with $\epsilon_r = 4.4$, with a height of 1.6mm. The length and width of the dielectric is taken as 25mm and 21mm. The radiating patch is placed on the top layer of the dielectric medium and the ring structure is placed on the bottom plane of the structure, fig4.

The structure is simulated using Ansoft-HFSS and the simulated result of the proposed prototype is shown in figure 5. From the simulated result, it can be observed that the proposed prototype operates in the frequency range 5.5GHz. The proposed prototype had a very less return loss of -28dB, which stands as an optimum value for the antenna to operate at the WLAN band. The prototype achieved a gain of 3.6dB, and an omnidirectional pattern, which are plotted in figures 6, respectively. From the figure 6, it can be seen that the proposed prototype radiates efficiently and the major lobe or main beam occurs at $\theta = 0^\circ$. Figure 6, represents the E-plane pattern. The radiation efficiency was achieved as 99% in the operating band of the prototype and is plotted. The voltage standing wave ratio being an important parameter for deciding an antenna's performance, it was found to be < 2 , from the achieved prototype and is plotted in figure 8.

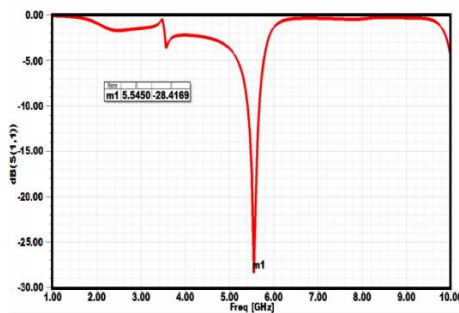


Figure 5: Simulated result of the inverted T-slot antenna.

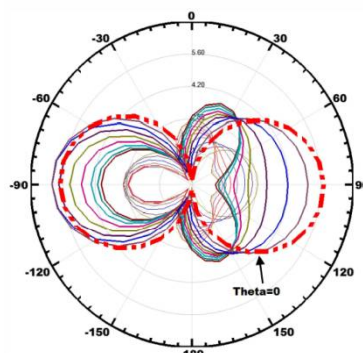


Figure 6: Simulated radiation pattern E-plane, where the major lobe occurs at $\theta = 0^\circ$.

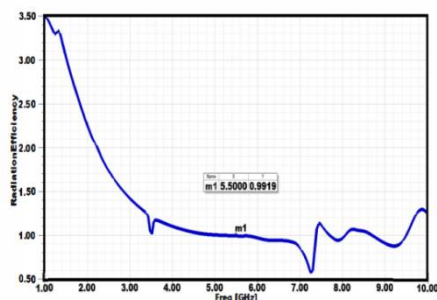


Figure 7: Plot for Radiation Efficiency at 5.5 GHz.

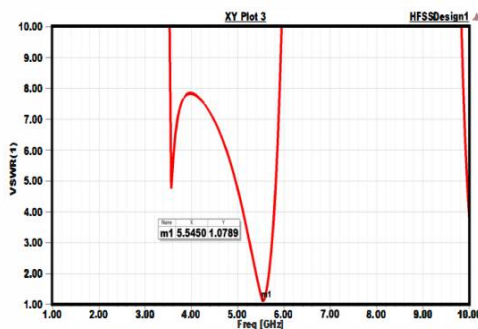


Figure 8: Simulated VSWR at frequency 5.5GHz.

VII. CONCLUSION

A metamaterial UWB inverted T-slotted antenna is proposed here with a reduced size than the conventional antennas. It achieved a size reduction of 11 % because of using SRR's in the structure to achieve metamaterial effect. The proposed antenna resonated at 5.5GHz, with a radiation efficiency of 9.9%, at the resonant frequency. The antenna achieved about 3dB gain, and the fractional bandwidth of about 21%, which stands as supporting feature of the antenna for being applicable for ultra wideband applications. The performance parameters like VSWR and reflection losses were analyzed in which the proposed antenna achieved 1.02, 1.22 (simulated & tested) and the reflection loss of about -28dB, -12dB (simulated & tested) respectively. The negative effects of the antenna were analyzed and are plotted, achieving both the permittivity and permeability values as negative. The proposed prototype was about 21mm x 25mm, which is of compact size when compared with the conventional design of antennas.

REFERENCES

- [1] Xu, F., Z.-X. Wang, X. Chen, and X.-A. Wang, "Dual band-notched UWB antenna based on spiral electromagnetic-bandgap structure," *Progress In Electromagnetics Research B*, Vol. 39, 393-409, 2012.
- [2] Tilanthe, P., P. C. Sharma, and T. K. Bandopadhyay, "A compact UWB antenna with dual band rejection," *Progress In Electromagnetics Research B*, Vol. 35, 389-405, 2011.
- [3] Khaled, E. E. M., A. A. R. Saad, and D. A. Salem, "Approximity-FED annular slot antenna with different band-notch manipulations for ultrawide band applications," *Progress In Electromagnetics Research B*, Vol. 37, 289-306, 2012.
- [4] Chen, H., Y. Ding, and D. S. Cai, "A CPW-fed UWB antenna with WiMAX/WLAN band-notched characteristics," *Progress In Electromagnetics Research*, Vol. 25, 163-173, 2011.
- [5] Enoch, Stefan; Tayeb, G; Sabouroux, P; Guerin, N; Vincent, P "A Metamaterial for Directive Emission" *Phys.Rev. Lett.* doi: IO.II03/PhysRevLett.89.213902, Sep 2009.
- [6] D. R. Smith, J. B. Pendry and M. C. K. Wiltshire, *Science*, 2004, 305, 788-792.
- [7] S. A. Ramakrishna, *Rep. Prog. Phys.*, 2005, 68, 449-521.
- [8] L. Fok, M. Ambati and X. Zhang, *MRS Bull.*, 2008, 8, 3998-4001.
- [9] N. Fang, D. J. Xi, J. Y. Xu, M. Ambati, W. Srituravanich, C. Sun and X. Zhang, *Nat. Mater.*, 2006, 5, 452-456.

International Journal of Innovative Research in Science, Engineering and Technology

(An ISO 3297: 2007 Certified Organization)

Vol. 5, Issue 6, June 2016

- [10] J. B. Pendry, A. J. Holden, D. J. Robbins and W. J. Stewart, IEEE Trans. Microwave Theory Tech., 1999, 47, 2075–2084.
- [11] Zhang, S., et al., Phys. Rev. Lett. (2005) 95, 137404
- [12] Enkrich, C., et al., Phys. Rev. Lett. (2005) 95, 203901
- [13] Ramakrishna, S. A., (2006), private communication
- [14] Ramakrishna, S. A., Rep. Prog. Phys. (2005) 68, 449
- [15] Focus Issue on Negative Refraction, New J. Phys. (2005) 7, 158, 191, 210, 220, 223, 255
- [16] Focus Issue on Metamaterials, J. Opt. Soc. Am. B (2006) 23, 386
- [17] Caloz, C., and Itoh, T., Electromagnetic Metamaterials: Transmission Line Theory and Microwave Applications, Wiley-IEEE Press, New Jersey, USA, (2005)
- [18] Eleftheriades, G. V., and Balmain, K. G., Negative Refraction Metamaterials: Fundamental Principles and Applications, Wiley-IEEE Press, New Jersey, USA, (2005)
- [19] Engheta, N., and Ziolkowski, R. W., (eds.), Electromagnetic Metamaterials: Physics and Engineering Explorations, Wiley-IEEE Press, New Jersey, USA, (2006)
- [20] Hecht, E., Optics, 4th edition, Addison-Wesley, Massachusetts, USA, (2001)
- [21] For a modern and complete investigation of refraction in EM-MMs see: Grzegorzczuk, T. M., et al., IEEE Trans. Microw. Theory Tech. (2005) 53, 1443
- [22] Foteinopoulou, S., et al., Phys. Rev. Lett. (2003) 90, 107402
- [23] Parimi, P. V., et al., Nature (2003) 426, 404
- [24] Luo, C., et al., Phys. Rev. B (2002) 65, 201104